
BAYESIAN GEOGRAPHICALLY WEIGHTED REGRESSION USING FUSED LASSO PRIOR

Toshiki Sakai

Graduate School of Culture and Information Science, Doshisha University
toshikisakai0711@gmail.com

Jun Tsuchida

Faculty of Data Science, Kyoto Women's University

Hiroshi Yadohisa

Faculty of Culture and Information Science, Doshisha University

ABSTRACT

A main purpose of spatial data analysis is to predict the objective variable for the unobserved locations. Although Geographically Weighted Regression (GWR) is often used for this purpose, estimation instability proves to be an issue. To address this issue, Bayesian Geographically Weighted Regression (BGWR) has been proposed. In BGWR, by setting the same prior distribution for all locations, the coefficients' estimation stability is improved. However, when observation locations' density is spatially different, these methods do not sufficiently consider the similarity of coefficients among locations. Moreover, the prediction accuracy of these methods becomes worse. To solve these issues, we propose Bayesian Geographically Weighted Sparse Regression (BGWSR) that uses Bayesian Fused Lasso for the prior distribution of the BGWR coefficients. Constraining the parameters to have the same values at adjacent locations is expected to improve the prediction accuracy at locations with a low number of adjacent locations. Furthermore, from the predictive distribution, it is also possible to evaluate the uncertainty of the predicted value of the objective variable. By examining numerical studies, we confirmed that BGWSR has better prediction performance than the existing methods (GWR and BGWR) when the density of observation locations is spatial difference. Finally, the BGWSR is applied to land price data in Tokyo. Thus, the results suggest that BGWSR has better prediction performance and smaller uncertainty than existing methods.

Keywords Hierarchical Bayesian Model · Laplace Prior · Spatial Heterogeneity

1 Introduction

Spatial data denote data that comprise individual values and the spatial location information where they were observed. The application of spatial data, such as mapping to understand visual features and creating hazard maps for disasters (Fischer and Getis, 2010), is used in various research fields. When we obtain spatial data, we sometimes set objective variables and covariates for the variables obtained. The purposes of analyzing such spatial data include visualization of spatial data, classification and division of space, and prediction of the value of the objective variable (e.g., Jena et al., 2023; Wang et al., 2023). The prediction of the objective variable's value is important in analyzing spatial data because there are many unobserved locations for the objective variables in many cases.

There are two main ways to predict the objective variable. The first applies to the spatial data containing only the objective variable. The methods used in this case include Kriging (Krige, 1951), inverse distance weighting (Bailey et al., 1995), and spline (Cline, 1973). For example, Kriging predicts the value of the objective variable at the prediction location using a weighted average of the available objective variable data. The second applies to the spatial data containing covariates in addition to the objective variable. The methods used in this case include Kriging with an

external drift (Ahmed and De Marsily, 1987). One of the most frequently used methods is Geographically Weighted Regression (GWR) (Brunsdon et al., 1996; Fotheringham et al., 2003). GWR is based on linear regression and assumes a multiple regression model with different coefficients for each location. Further, it assumes that the values of the coefficients are similar for locations close to each other—the method assumes spatial autocorrelation in the coefficients. In Yu et al. (2007), GWR is used to investigate the relationship among housing prices, floor space, and age of the house in Milwaukee, Wisconsin, in the United States. In Koh et al. (2020), GWR is used to investigate the relationship among Nitrate concentrations, land use, and precipitation in South Korea.

Notably, when applying GWR to real data, the estimation of coefficients becomes unstable when the number of observation locations is small (LeSage, 2004; Subedi et al., 2018) because of the small number of observations used to estimate the coefficients. In extreme cases, for estimation coefficients, we could use only one or two locations, and the solution of the weighted least squared method may not be uniquely determined. To solve this issue, Bayesian Geographically Weighted Regression (BGWR) has been proposed (LeSage, 2004). BGWR is a method for estimating parameters of GWR within the framework of Bayesian statistics. Specifically, parameters such as coefficients are assumed to follow a certain probability distribution, and the estimator is the expected value of the posterior distribution calculated by using the data. Setting a common prior distribution for all locations allows for a stable estimation of coefficients when the number of locations is small, as information from the prior distribution becomes more weighted in the estimation. Additionally, BGWR allows us to evaluate the instability of the objective variable's predicted value because the predicted value's credibility is calculated by the predictive distribution.

However, these methods sometimes estimate considerably different coefficients for adjacent locations. For example, two close yet adjacent locations do not share the same location for estimation. In such a situation, the similarity of the coefficients at adjacent locations, as assumed by spatial autocorrelation, cannot be fully captured because the coefficients are estimated using completely different data (Fotheringham et al., 2017).

To resolve this issue, we propose a novel method by using the idea of Fused Lasso (Tibshirani et al., 2005). Fused Lasso penalizes the absolute value of the difference between the coefficients at adjacent locations, making it easier to obtain the same estimated value of the coefficient at adjacent locations. For example, Li and Sang (2019) and Zhong et al. (2023) use Fused Lasso penalties to consider the similarity of the coefficient of regression and show improved prediction performance compared to the GWR. Hence, the proposed method—Bayesian Geographically Weighted Sparse Regression (BGWSR)—combines BGWR and Bayesian Fused Lasso Kyung et al. (2010) and is expected to obtain similar estimates of coefficients between adjacent locations. This is because the Laplace distribution is set for the difference in coefficients between adjacent locations, and the difference between adjacent locations is easily estimated as 0. Moreover, as BGWSR can consider the similarity between adjacent locations, it is expected to improve the prediction accuracy of coefficients and objective variables compared to existing methods.

In BGWR and GWR, when observation locations are obtained from a spatially heterogeneous environment (i.e., there are areas whose density is sparse and dense), the estimation of coefficients and predictions for the observed locations may be less accurate. For example, if adjacent locations are defined as extremely close in distance, the number of observation locations used to estimate the coefficients will not be sufficient in areas where the density of observation locations is sparse, and the resulting estimation will be unstable. Therefore, for stable estimation, it is necessary to have excessive information in the prior distribution. Nevertheless, when adjacent locations are defined as distant locations, the estimated values of the coefficients may be the same for most locations because the same data are shared by many locations and the penalty of Fused Lasso. Furthermore, in areas with dense observation locations, it is necessary to define adjacent locations as those close to each other to consider rapid changes adequately. By introducing a prior distribution for setting the width of each location to be an adjacent location, it is expected that the appropriate adjacent location will be determined for all locations. This allows for a trade-off between the breadth of the definition of the adjacency points and the strength of the to-be-determined Fused Lasso penalty so that the estimation performance is better for each location. Therefore, introducing this prior is expected to improve the prediction accuracy of coefficients and objective variables even when locations are spatially heterogeneous.

This paper is organized as follows. In Section 2, we introduce the proposed method and other predictive algorithms. In Section 3, we evaluate the numerical performance of the proposed methods together with some existing methods through numerical studies. In Section 4, we demonstrate the proposed method through spatial regression modeling of the land prices in the Tokyo metropolitan area. Finally, Section 5 summarizes our main conclusions and identifies areas where further research is necessary.

2 Bayesian Geographically Weighted Sparse Regression (BGWSR)

2.1 Model

This section describes the model for Bayesian estimation of the BGWSR. Let $D \subset \mathbb{R}^2$ be the region to be analyzed, and let $\mathbf{s}_i = (s_{1i}, s_{2i})' \in D$ be the i -th location. Suppose a set of spatial data $(x(\mathbf{s}_i), y(\mathbf{s}_i))$ is observed locations $\mathbf{s}_1, \dots, \mathbf{s}_n \in D$, where the objective variable $y(\mathbf{s}_i)$ is assumed to be spatially correlated, and $\mathbf{x}(\mathbf{s}_i) = (x_1(\mathbf{s}_i), \dots, x_p(\mathbf{s}_i))'$ is the p -dimensional vector of covariates at the location \mathbf{s}_i .

$$y(\mathbf{s}_i) = \mathbf{x}(\mathbf{s}_i)' \boldsymbol{\beta}(\mathbf{s}_i) + \varepsilon(\mathbf{s}_i).$$

We assume that $\boldsymbol{\beta}(\mathbf{s}_i)$ is the coefficient and that the error terms $\varepsilon(\mathbf{s}_i)$ follow a Normal distribution $N(0, \sigma^2)$ ($\sigma^2 > 0$) independent of each other.

To estimate the coefficients, we consider that the coefficients are described by n -dimensional vectors. Let $\boldsymbol{\beta}_k$ be a vector of coefficients whose i -th elements are the coefficient $\beta_k(\mathbf{s}_i)$ ($k = 1, 2, \dots, p$), and be defined as $\mathbf{y}_k = \mathbf{X}_k \boldsymbol{\beta}_k + \boldsymbol{\varepsilon}_k$, where $\boldsymbol{\varepsilon}_k \sim MN(\mathbf{0}_n, \sigma^2 \mathbf{I}_n/p)$, and \mathbf{I}_n is n -dimensional identity matrix. $MN(\boldsymbol{\mu}, \boldsymbol{\Sigma})$ denotes the Multivariate Normal distribution of the mean vector $\boldsymbol{\mu}$ and covariance matrix $\boldsymbol{\Sigma}$. The \mathbf{X}_k is an n -dimensional diagonal matrix and $\mathbf{X}_k = \text{diag}\{x_k(\mathbf{s}_1), x_k(\mathbf{s}_2), \dots, x_k(\mathbf{s}_n)\} \in \mathbb{R}^{n \times n}$. Using these terms, the $\mathbf{y} = (y(\mathbf{s}_i))$ is represented as $\mathbf{y} = \sum_{k=1}^p \mathbf{y}_k = \sum_{k=1}^p \mathbf{X}_k \boldsymbol{\beta}_k + \boldsymbol{\varepsilon}_k$. The model for estimating the parameters at location \mathbf{s}_i is given as follows based on BGWR (LeSage, 2004).

$$\mathbf{W}(\mathbf{s}_i) \mathbf{y}_k = \mathbf{W}(\mathbf{s}_i) \mathbf{X}_k \boldsymbol{\beta}_k + \boldsymbol{\varepsilon}_k. \quad (1)$$

$\mathbf{W}(\mathbf{s}_i)$ is an n -dimensional diagonal matrix, and $\mathbf{W}(\mathbf{s}_i) = \text{diag}\{w_1(\mathbf{s}_i), w_2(\mathbf{s}_i), \dots, w_n(\mathbf{s}_i)\}$ and $w_j(\mathbf{s}_i) (\geq 0; j = 1, 2, \dots, n)$ are weights determined by the distance between two locations \mathbf{s}_i and \mathbf{s}_j .

For handling the spatial autocorrelation of coefficients, the Fused Lasso Prior is selected as the prior distribution of the coefficients in BGWSR. The following distribution is set as the prior distribution of the coefficient β_k ($k = 1, 2, \dots, p$) for the k -th covariates.

$$\begin{aligned} \boldsymbol{\beta}_k | \sigma^2, S, N, C, \lambda_{k,1}, \lambda_{k,2} \sim & (\sigma^2)^{-\frac{2n + \sum_{i=1}^n n_i}{4}} \prod_{i=1}^n \text{Laplace} \left(\frac{\beta_k(\mathbf{s}_i)}{\sqrt{\sigma^2}} \middle| 0, \lambda_{k,1} \right) \\ & \times \prod_{(i,j) \in C} \text{Laplace} \left(\frac{\beta_k(\mathbf{s}_i) - \beta_k(\mathbf{s}_j)}{\sqrt{\sigma^2}} \middle| 0, \lambda_{k,2} \right), \end{aligned} \quad (2)$$

where $\text{Laplace}(x | \mu, b)$ denotes the Laplace distribution of mean μ and scale parameter b with x as a random variable. S is the set of the observed locations and $S = \{\mathbf{s}_1, \mathbf{s}_2, \dots, \mathbf{s}_n\} \subset D$. N is the set of the number of adjacent locations n_i at location \mathbf{s}_i , where $N = \{n_1, n_2, \dots, n_n\}$. C is a set of pairs of adjacent locations, and $(i, j) \in C$ indicates that two locations $\mathbf{s}_i, \mathbf{s}_j$ are spatially close to each other. $\lambda_{k,1}, \lambda_{k,2}$ are parameters that determine the strength of the shrinkage. For example, the following is obtained.

$$C = \{(i, j) \mid w_j(\mathbf{s}_i) > 0\}.$$

The first term on the right-hand side of the equation (2) is a Laplace distribution with mean 0 for the coefficient at each location based on the idea of Bayesian Lasso (Park and Casella, 2008). The role of this term is to shrink the coefficient to 0 regardless of location. As it tends to shrink to 0 of the estimated value of the coefficient at a location with a small size adjacent set to 0, the estimation is more numerically stable than GWR. The second term on the right side of the equation (2) is based on the idea of Bayesian Fused Lasso (Kyung et al., 2010), setting a Laplace distribution with mean 0 for the difference of coefficients at adjacent locations. This allows us to estimate similar coefficients for adjacent locations.

As the coefficients $\boldsymbol{\beta}_k$ have a Laplace distribution for the prior distribution, the full conditional distribution for Gibbs sampling cannot be derived explicitly without modification. We apply parameter augmentation (Andrews and Mallows, 1974). For calculating the posterior distribution, the prior distribution of the coefficient $\boldsymbol{\beta}_k$ can be rewritten using the parameter $\tau_{k,i}^2, \omega_{k,i,j}^2$ ($i = 1, 2, \dots, n; j = 1, 2, \dots, n, i \neq j; k = 1, 2, \dots, p$) as follows, where $\tau_{k,i}^2 > 0, \omega_{k,i,j}^2 > 0$.

$$\begin{aligned} \boldsymbol{\beta}_k | \sigma^2, T_k, \Omega_k & \sim MN(\mathbf{0}_n, \sigma^2 \boldsymbol{\Sigma}_k^{-1}), \\ T_k | \lambda_{k,1}^2 & \sim \prod_{i=1}^n \frac{\lambda_{k,1}^2}{2} \exp \left\{ -\frac{\lambda_{k,1}}{2} \tau_{k,i}^2 \right\}, \\ \Omega_k | \lambda_{k,2}^2 & \sim \prod_{(i,j) \in C} \frac{\lambda_{k,2}^2}{2} \exp \left\{ -\frac{\lambda_{k,2}}{2} \omega_{k,i,j}^2 \right\}. \end{aligned}$$

Here, $T_k = \{\tau_{k,1}^2, \tau_{k,2}^2, \dots, \tau_{k,n}^2\}$, $\Omega_k = \{\omega_{k,1,2}^2, \omega_{k,1,3}^2, \dots, \omega_{k,n-1,n}^2\}$ and $\omega_{k,i,j}^2 = \omega_{k,j,i}^2$ ($k = 1, 2, \dots, p$). Let $\sigma^2 \Sigma_k^{-1}$ be the covariance matrix of the coefficients defined as

$$(\Sigma_k^{-1})_{ij} = \begin{cases} \frac{1}{\tau_{k,i}^2} + \sum_{(i,\ell) \in C_i} \frac{1}{\omega_{k,i,\ell}^2} & (i = j) \\ -\frac{1}{\omega_{k,i,j}^2} & (i \neq j, (i, j) \in C) \\ 0 & (\text{otherwise}), \end{cases}$$

where $C_i \subset C$ is a set comprising only pairs of locations adjacent to \mathbf{s}_i .

Based on Kyung et al. (2010), the models for the other parameters are set as

$$\begin{aligned} \lambda_{k,1}^2 | r_1, q_1 &\sim \text{Gamma}(r_1, q_1), & \lambda_{k,2}^2 | r_2, q_2 &\sim \text{Gamma}(r_2, q_2), \\ \sigma^2 | r, q &\sim \text{IGamma}\left(\frac{r}{2}, \frac{q}{2}\right), & w_j(\mathbf{s}_i) | h &= f(d_{ij} | h), \end{aligned}$$

where $\text{Gamma}(a, b)$, $\text{IGamma}(a, b)$ denote the gamma distribution and Inverse Gamma distribution with shape parameter a and reciprocal scale parameter b . Meanwhile r, q, r_1, q_1, r_2, q_2 are hyperparameters determined by the analyst. The function $f(d_{ij} | h)$ determines the weights of two locations $\mathbf{s}_i, \mathbf{s}_j$ with the distance d_{ij} as an argument. For example, the following equation is used.

$$f(d_{ij} | h) = \begin{cases} 1 - \left(\frac{d_{ij}}{h}\right)^2 & (\|\mathbf{s}_i - \mathbf{s}_j\| < h) \\ 0 & (\text{otherwise}) \end{cases}.$$

h is a parameter that determines the degree of spatial correlation. It may be determined by the analyst based on domain knowledge, or it can be incorporated as a model. For example, based on Boehm Vock et al. (2015); Ma et al. (2021), we have

$$h | a \sim \text{U}(0, a), \quad (3)$$

where $\text{U}(0, a)$ represents a Uniform distribution with lower limit 0 and upper limit a , where a is the hyperparameter determined by the analyst. For example, the maximum distance between locations in a region is set as a . Sampling methods of the posterior distribution of h include the Metropolis–Hastings Algorithm (MH method) (Ma et al., 2021). The method of determining the optimal adjacency for each location is described in 2.3.

2.2 Parameter estimation

The probability density function of the simultaneous posterior distributions of the parameters for BGWSR has a complex form. Therefore, Gibbs sampling and MH method are used to estimate the posterior distribution of the parameters. For $\beta_k, \sigma^2, \lambda_{k,1}^2, \lambda_{k,2}^2$, Gibbs sampling is used because the probability density function of the conditional distribution can be derived explicitly. For the parameter h , we use the MH method based on Ma et al. (2021).

First, We show the conditional distribution for Gibbs sampling. The full conditional distribution of the coefficients β_k is given as follows,

$$\begin{aligned} \beta_k | \mathbf{X}_k, \mathbf{y}_k, \Sigma_k^{-1}, W, \sigma^2, T_k, \Omega_k \\ \sim \text{MN} \left(\left(\mathbf{X}_k \sum_{i=1}^n (\mathbf{W}(\mathbf{s}_i))^2 \mathbf{X}_k + \Sigma_k^{-1} \right)^{-1} \mathbf{X}_k \sum_{i=1}^n (\mathbf{W}(\mathbf{s}_i))^2 \mathbf{y}_k, \sigma^2 \left(\mathbf{X}_k \sum_{i=1}^n \mathbf{W}(\mathbf{s}_i)^2 \mathbf{X}_k + \Sigma_k^{-1} \right) \right), \end{aligned}$$

where W denotes the set of weight matrices for all locations, and $W = \{\mathbf{W}(\mathbf{s}_1), \mathbf{W}(\mathbf{s}_2), \dots, \mathbf{W}(\mathbf{s}_n)\}$. The conditional distribution of the parameters T_k, Ω_k added by parameter augmentation is as follows.

$$\begin{aligned} \frac{1}{\tau_{k,i}^2} | \beta_k(\mathbf{s}_i), \sigma^2, \lambda_{k,1} &\sim \text{IGauss} \left(\sqrt{\frac{\lambda_{k,1}^2 \sigma^2}{\beta_k(\mathbf{s}_i)^2}}, \lambda_{k,1}^2 \right), \\ \frac{1}{\omega_{k,i,j}^2} | \beta_k(\mathbf{s}_i), \beta_k(\mathbf{s}_j), \sigma^2, \lambda_{k,2} &\sim \text{IGauss} \left(\sqrt{\frac{\lambda_{k,2}^2 \sigma^2}{(\beta_k(\mathbf{s}_i) - \beta_k(\mathbf{s}_j))^2}}, \lambda_{k,2}^2 \right), \end{aligned}$$

where $\text{IGauss}(\mu, \lambda)$ denotes the Inverse Gaussian distribution with mean μ and shape parameter λ .

The full conditional distribution of the parameters σ^2 , $\lambda_{k,1}$, $\lambda_{k,2}$ is given below. We discuss the parameter h in the next section.

$$\begin{aligned} \sigma^2 | \mathbf{W}(\mathbf{s}_i) \mathbf{y}_k, \mathbf{W}(\mathbf{s}_i) \mathbf{X}_k, \boldsymbol{\beta}_k &\sim \text{IGamma}(r_*, q_*), \\ r_* &= r + \frac{pn^2}{2}, \\ q_* &= q + \frac{\sum_{i=1}^n \sum_{k=1}^p \|\mathbf{W}(\mathbf{s}_i) \mathbf{y}_k - \mathbf{W}(\mathbf{s}_i) \mathbf{X}_k \boldsymbol{\beta}_k\|^2}{2}, \\ \lambda_{k,1}^2 | \mathbf{y}_k, \mathbf{X}_k, \boldsymbol{\beta}_k, \sigma^2, T_k, \Omega_k &\sim \text{Gamma}(r_1^*, q_1^*), \\ r_1^* &= r_1 + n, \\ q_1^* &= q_1 + \frac{1}{2} \sum_{i=1}^n \tau_{k,i}^2, \\ \lambda_{k,2}^2 | \mathbf{y}_k, \mathbf{X}_k, \boldsymbol{\beta}_k, \sigma^2, T_k, \Omega_k &\sim \text{Gamma}(r_2^*, q_2^*), \\ r_2^* &= r_2 + \frac{1}{2} \sum_{i=1}^n n_i, \\ q_2^* &= q_2 + \frac{1}{2} \sum_{(i,j) \in C} \omega_{k,i,j}^2. \end{aligned}$$

2.3 Adjacency estimation

In BGWSR, BGWR, and GWR, the parameter h , which determines the range of locations to be adjacent, is the same for all locations. Therefore, these methods implicitly assume that the observed locations are obtained uniformly within the region. However, actual data may include dense areas with many locations and sparse areas with few locations. In an area with sparse observation locations, numerous adjacent locations are required to have adequate data for the coefficient estimation. Nevertheless, in an area with dense locations, it is necessary to reduce the range of neighboring locations to capture local changes in the coefficients successfully. Therefore, we consider the range of adjacent locations for each location. Specifically, the MH method is used for sampling, allowing the parameters responsible for determining the range of adjacency to vary from one location to another. The sampling scheme of h in Equation (3) is the special case of this sampling scheme.

We set the prior distribution of the parameter $h(\mathbf{s}_i)$ that determines the adjacent location at location \mathbf{s}_i as

$$h(\mathbf{s}_i) | a \stackrel{\text{i.i.d.}}{\sim} \text{U}(0, a),$$

where $h(\mathbf{s}_i)$ is a parameter that determines the adjacency range at location \mathbf{s}_i . By setting $h(\mathbf{s}_i)$ as a different parameter for each location, we can expect to estimate a smaller adjacency range in areas with dense observation locations and large local changes in the coefficients. Subsequently, in areas with sparse observation locations, a large adjacency range is expected to be estimated.

We use the MH method to sample the parameter $h(\mathbf{s}_i)$. The sampling procedure for $h(\mathbf{s}_i)$ at location \mathbf{s}_i using the MH method is as follows.

1. We use the Normal distribution as the proposal distribution. A new $h(\mathbf{s}_i)$ candidate $h_{\text{prop}}(\mathbf{s}_i)$ is sampled using the proposal distribution as follows.

$$h_{\text{prop}}(\mathbf{s}_i) | \sigma_h^2 \sim \text{N}(h_{\text{cur}}(\mathbf{s}_i), \sigma_h^2).$$

In the above, $h_{\text{cur}}(\mathbf{s}_i)$ is the sampled $h(\mathbf{s}_i)$ before the update, and σ_h^2 is the hyperparameter representing the variance of the proposal distribution.

2. Decide whether to accept $h_{\text{prop}}(\mathbf{s}_i)$ based on the posterior probability. Specifically, calculate α as defined in the following equation.

$$\begin{aligned}\alpha &= \min \left(1, \frac{p(h_{\text{prop}}(\mathbf{s}_i)|\text{data})}{p(h_{\text{cur}}(\mathbf{s}_i)|\text{data})} \right) \\ &= \min \left(1, \frac{\prod_{k=1}^p p(\mathbf{W}_{h_{\text{prop}}(\mathbf{s}_i)}(\mathbf{s}_i)\mathbf{y}_k | \mathbf{W}_{h_{\text{prop}}(\mathbf{s}_i)}(\mathbf{s}_i)\mathbf{X}_k, \boldsymbol{\beta}_k, \sigma^2)}{\prod_{k=1}^p p(\mathbf{W}_{h_{\text{cur}}(\mathbf{s}_i)}(\mathbf{s}_i)\mathbf{y}_k | \mathbf{W}_{h_{\text{cur}}(\mathbf{s}_i)}(\mathbf{s}_i)\mathbf{X}_k, \boldsymbol{\beta}_k, \sigma^2)} \right) \\ &= \min \left(1, \frac{\exp \left\{ -\frac{1}{2\sigma^2} \left\| \sum_{k=1}^p (\mathbf{W}_{h_{\text{prop}}(\mathbf{s}_i)}(\mathbf{s}_i)\mathbf{y}_k - \mathbf{W}_{h_{\text{prop}}(\mathbf{s}_i)}(\mathbf{s}_i)\mathbf{X}_k\boldsymbol{\beta}_k) \right\|^2 \right\}}{\exp \left\{ -\frac{1}{2\sigma^2} \left\| \sum_{k=1}^p (\mathbf{W}_{h_{\text{cur}}(\mathbf{s}_i)}(\mathbf{s}_i)\mathbf{y}_k - \mathbf{W}_{h_{\text{cur}}(\mathbf{s}_i)}(\mathbf{s}_i)\mathbf{X}_k\boldsymbol{\beta}_k) \right\|^2 \right\}} \right).\end{aligned}$$

In the above, $\mathbf{W}_h(\mathbf{s}_i)$ is the matrix $\mathbf{W}(\mathbf{s}_i)$ representing the weights of the neighbors when $h = h$.

3. Using $u \sim U(0, 1)$, update h as follows.

$$h_{\text{cur}}(\mathbf{s}_i) = \begin{cases} h_{\text{prop}}(\mathbf{s}_i) & (u < \alpha) \\ h_{\text{cur}}(\mathbf{s}_i) & (\text{otherwise}) \end{cases}.$$

Using these, the sampling method for BGWSR parameter estimation is represented by the following Algorithm 1. Here \mathbf{y} , \mathbf{X} , \mathbf{B} denote the set of objective variable vectors, the set of explanatory variable matrices, and the set of coefficient vectors, respectively, $\mathbf{y} = \{\mathbf{y}_1, \mathbf{y}_2, \dots, \mathbf{y}_p\}$, $\mathbf{X} = \{\mathbf{X}_1, \mathbf{X}_2, \dots, \mathbf{X}_p\}$, $\mathbf{B} = \{\boldsymbol{\beta}_1, \boldsymbol{\beta}_2, \dots, \boldsymbol{\beta}_p\}$.

Algorithm 1: Algorithm for BGWSR parameter sampling

Input: $\mathbf{s}_i, X, y, r, q, r_1, q_1, r_2, q_2, \sigma_h^2, t_{\text{max}}$ ($i = 1, 2, \dots, n; k = 1, 2, \dots, p$)

Output: \hat{B}

- 1: Initialize $\boldsymbol{\beta}_k^{(0)}, T_k^{(0)}, \Omega_k^{(0)}, \sigma^{2(0)}, \lambda_{k,1}^{(0)}, \lambda_{k,2}^{(0)}, h(\mathbf{s}_i)^{(0)}$ ($i = 1, 2, \dots, n; k = 1, 2, \dots, p$).
 - 2: Initialize $\mathbf{W}^{(0)}$ using $w_j(\mathbf{s}_i)|h(\mathbf{s}_i)^{(0)}$.
 - 3: Initialize $B^{(0)}$ using $\boldsymbol{\beta}_1^{(0)}, \boldsymbol{\beta}_2^{(0)}, \dots, \boldsymbol{\beta}_p^{(0)}$.
 - 4: Initialize $\Sigma_k^{-1(0)}$ using $T_k^{(0)}, \Omega_k^{(0)}$.
 - 5: **for** $t = 0, 1, \dots, t_{\text{max}}$ **do**
 - 6: **for** ($k = 1, 2, \dots, p$) **do**
 - 7: Sampling $\boldsymbol{\beta}_k^{(t+1)} \sim \pi(\boldsymbol{\beta}_k | \mathbf{X}_k, \mathbf{y}_k, W^{(t)}, \sigma^{2(t)}, \Sigma_k^{-1(t)})$.
 - 8: **end for**
 - 9: Update $B^{(t+1)}$ using $\boldsymbol{\beta}_1^{(t+1)}, \boldsymbol{\beta}_2^{(t+1)}, \dots, \boldsymbol{\beta}_p^{(t+1)}$.
 - 10: **for** $k=1, 2, \dots, p$ **do**
 - 11: Sampling $T_k^{(t+1)} \sim \pi(T_k | \boldsymbol{\beta}_k^{(t+1)}, \sigma^{2(t)}, \lambda_{k,1}^{(t)})$.
 - 12: Sampling $\Omega_k^{(t+1)} \sim \pi(\Omega_k | \boldsymbol{\beta}_k^{(t+1)}, \sigma^{2(t)}, \lambda_{k,2}^{(t)})$.
 - 13: Update $\Sigma_k^{-1(t)}$ using $T_k^{(t)}, \Omega_k^{(t)}$.
 - 14: **end for**
 - 15: Sampling $\sigma^{2(t+1)} \sim \pi(\sigma^2 | X, y, B^{(t+1)}, W^{(t)}, r, q)$.
 - 16: **for** $k=1, 2, \dots, p$ **do**
 - 17: Sampling $\lambda_{k,1}^{2(t+1)} \sim \pi(\lambda_{k,1}^2 | T_k^{(t+1)}, r_1, q_1)$.
 - 18: Sampling $\lambda_{k,2}^{2(t+1)} \sim \pi(\lambda_{k,2}^2 | \Omega_k^{(t+1)}, r_2, q_2)$.
 - 19: Sampling $h(\mathbf{s}_i)^{(t+1)} \propto \pi(h(\mathbf{s}_i) | y, X, B^{(t+1)}, \sigma^{2(t+1)}, \sigma_h^2)$ by MH method.
 - 20: **end for**
 - 21: Update $W^{(t+1)}$ using $w_j(\mathbf{s}_i)|h(\mathbf{s}_i)^{(t+1)}$.
 - 22: **end for**
-

2.4 Objective variable Prediction

The weight parameter $w_j(\mathbf{s}_{i^*})$ at any prediction location $\mathbf{s}_{i^*} \in D$ is given by

$$w_j(\mathbf{s}_{i^*}) = \begin{cases} 1 - \left(\frac{d_{i^*j}}{h(\mathbf{s}_j)} \right)^2 & (d_{i^*j} < h(\mathbf{s}_j)) \\ 0 & (\text{otherwise}) \end{cases}, \quad (j = 1, 2, \dots, n). \quad (4)$$

Using this, we predict the coefficient $\beta(\mathbf{s}_{i^*}) = (\beta_1(\mathbf{s}_{i^*}), \beta_2(\mathbf{s}_{i^*}), \dots, \beta_p(\mathbf{s}_{i^*}))'$ at the prediction location \mathbf{s}_{i^*} by the following formula.

$$\widehat{\beta}(\mathbf{s}_{i^*}) = \sum_{j=1}^n w_j(\mathbf{s}_{i^*})\beta(\mathbf{s}_j). \quad (5)$$

Using $\widehat{\beta}(\mathbf{s}_{i^*})$, $\mathbf{x}(\mathbf{s}_{i^*})$, we predict the objective variable $y(\mathbf{s}_{i^*})$ at the prediction location \mathbf{s}_{i^*} with the following formula.

$$\widehat{y}(\mathbf{s}_{i^*}) = \mathbf{x}(\mathbf{s}_{i^*})'\widehat{\beta}(\mathbf{s}_{i^*}). \quad (6)$$

Therefore, the algorithm for predicting the coefficients and the objective variable at the prediction locations is given by algorithm 2, where n^* is the number of locations predicted.

Algorithm 2: Algorithm for predicting coefficients and objective variables at the prediction location by BGWSR

Input: $\mathbf{s}_i, \mathbf{s}_{i^*}, \mathbf{X}_k, \mathbf{X}_k^*, \mathbf{y}_k, r, q, r_1, q_1, r_2, q_2, \sigma_h^2, t_{\max}$ ($i = 1, 2, \dots, n; i^* = 1, 2, \dots, n^*; k = 1, 2, \dots, p$)

Output: $\widehat{\beta}(\mathbf{s}_{i^*}), \widehat{y}(\mathbf{s}_{i^*})$ ($i^* = 1, 2, \dots, n^*$)

```

1: for  $t = 0, 2, \dots, t_{\max}$  do
2:   for  $i^* = 1, 2, \dots, n^*$  do
3:     for  $j = 1, 2, \dots, n$  do
4:       Calculate  $w_j(\mathbf{s}_{i^*})^{(t)}$  from equation (4).
5:     end for
6:     Sampling  $\widehat{\beta}(\mathbf{s}_{i^*})^{(t)}$  from equation (5).
7:     Sampling  $\widehat{y}(\mathbf{s}_{i^*})^{(t)}$  from equation (6).
8:   end for
9: end for
```

3 Numerical studies

In this section, we describe the details and results of numerical studies conducted to evaluate the prediction performance of the proposed method.

3.1 Settings

In data generation, we first generated the location, followed by the data associated with the location. In all scenarios, we randomly generate $n = 1000$ spatial locations $\mathbf{s}_1, \mathbf{s}_2, \dots, \mathbf{s}_n$ in the square domain $[-1, 1] \times [0, 2]$ as follows.

$$\mathbf{s}_i = (s_{i1}, s_{i2})', \quad s_{i1} \stackrel{\text{i.i.d.}}{\sim} \text{U}(-1, 1), \quad s_{i2} \stackrel{\text{i.i.d.}}{\sim} \text{U}(0, 2).$$

The objective variables and covariates are generated as follows, where $p = 3$.

$$y(\mathbf{s}_i) = \sum_{k=1}^p x_k(\mathbf{s}_i)\beta_k(\mathbf{s}_i) + \varepsilon(\mathbf{s}_i), \quad i = 1, 2, \dots, n,$$

$$x_k(\mathbf{s}_i) \stackrel{\text{i.i.d.}}{\sim} \text{N}(0, 1), \quad i = 1, 2, \dots, n; k = 1, 2, \dots, p,$$

$$\varepsilon(\mathbf{s}_i) \stackrel{\text{i.i.d.}}{\sim} \text{N}(0, \sigma^2), \quad i = 1, 2, \dots, n.$$

The true values of the coefficients consider the following three structures of coefficients.

- (a1) The coefficients differ **smoothly**.
- (a2) The clusters are different in the left and right regions, and the coefficients within the clusters are the same.
- (a3) The clusters are different in the upper and lower regions, and the coefficients within the clusters are the same.

In (a1), the values are different for each location. The correlation of coefficients between adjacent locations is strong, and the coefficients have similar values. This structure of the coefficients is assumed for GWR and BGWR. In (a2) and

(a3), we assume a cluster structure depending on location so that spatially close locations belong to the same cluster and have the same coefficient values. We generated the true value of the coefficient at (a1) by

$$\boldsymbol{\beta}_k = (\beta_k(\mathbf{s}_1), \beta_k(\mathbf{s}_2), \dots, \beta_k(\mathbf{s}_n))' \sim \text{MN}(\beta_k^* \mathbf{1}_n, \sigma^2 \mathbf{H}), \quad k = 1, 2, \dots, p.$$

Here, we set the covariance matrix $\mathbf{H} \in \mathbb{R}^{n \times n}$ so that there is a correlation between adjacent locations,

$$\mathbf{H} = \begin{pmatrix} 1 & w_2(\mathbf{s}_1) & \cdots & w_n(\mathbf{s}_1) \\ w_1(\mathbf{s}_2) & 1 & \cdots & w_n(\mathbf{s}_2) \\ \vdots & \vdots & \ddots & \vdots \\ w_1(\mathbf{s}_n) & w_2(\mathbf{s}_n) & \cdots & 1 \end{pmatrix},$$

where $w_j(\mathbf{s}_i) = f(d_{ij}|h) = \exp\{-(d_{ij}^2/2h^2)\}$. We set the mean vector of coefficients $\boldsymbol{\beta}^* = (\beta_1^*, \beta_2^*, \beta_3^*)'$, the parameter of error variance σ^2 , and bandwidth h as described below.

$$\boldsymbol{\beta}^* = (1, 1, 1)', \quad \sigma^2 = 1^2, \quad h = 0.5.$$

We generated the true value of the coefficient at (a2) and (a3) by

$$\boldsymbol{\beta}(\mathbf{s}_i) = \boldsymbol{\beta}^{(g)}, \quad \mathbf{s}_i \in C_g.$$

Let C_g denote the set of locations belonging to the g -th cluster ($g = 1, 2$). We set the true values of the coefficients as follows.

$$\begin{aligned} \boldsymbol{\beta}^{(1)} &= (1, 1, 1)', \\ \boldsymbol{\beta}^{(2)} &= (2, 2, 2)'. \end{aligned}$$

We set the clusters of locations based on

$$\begin{aligned} \text{(a2)} : \quad \mathbf{s}_i &\in \begin{cases} C_1 & (s_{i1} \leq 0) \\ C_2 & (s_{i1} > 0), \end{cases} \\ \text{(a3)} : \quad \mathbf{s}_i &\in \begin{cases} C_1 & (s_{i2} \leq 0) \\ C_2 & (s_{i2} > 0). \end{cases} \end{aligned}$$

Figure 1 shows an example of coefficients generated in scenarios (a1), (a2) and (a3).

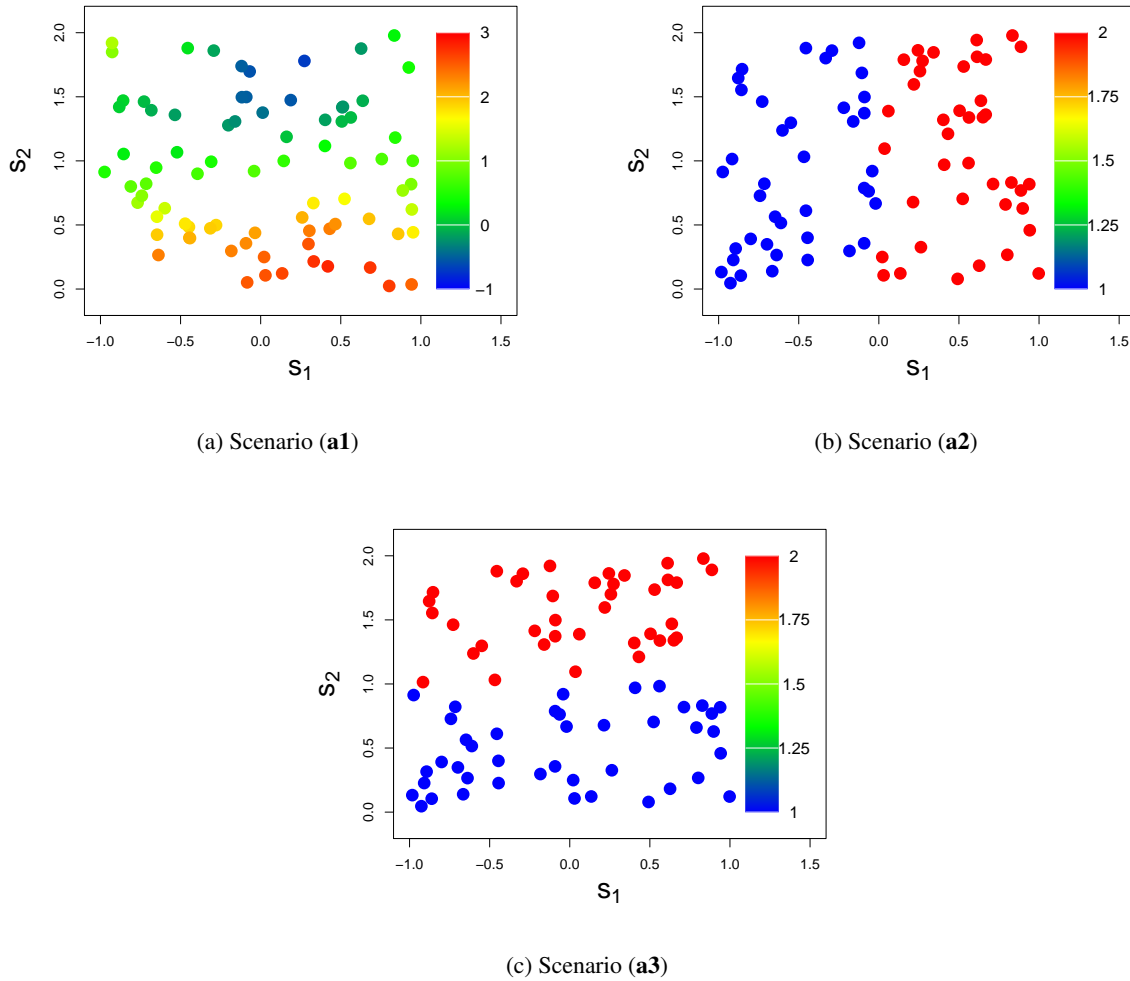


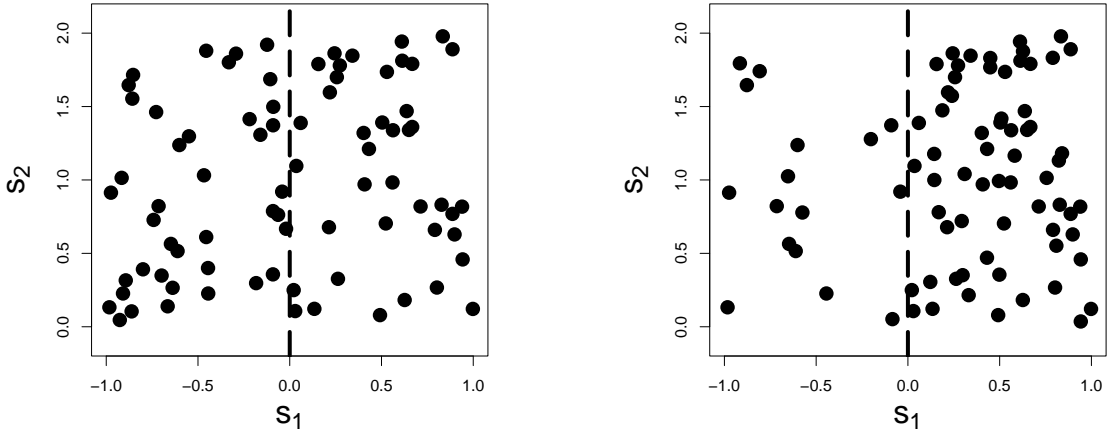
Figure 1: Examples of coefficients for each scenario

Next, we describe the division rule between observed and prediction locations. In the numerical studies, we extracted the predicted and observed locations from the generated locations. We randomly select 50 locations for the prediction. We set the number of observation locations to 100 and consider the following two conditions for the selection of observation locations.

- (b1) The observed location is **uniformly** obtained within the region.
- (b2) The observed location is **non-uniformly** obtained within the region.

In (b1), we randomly select locations from the generated data. In (b2), we extract locations from the generated data by setting the number of locations to 1 : 4 on the left and right sides of the entire region. (b1) is the situation assumed by GWR and BGWR. (b2) is the situation assumed by the BGWSR, where there are not many locations near a given point in the sparse left-hand area. Therefore, in GWR and BGWSR, the estimated coefficients are expected to differ among adjacent locations. Figure 2 shows an example of locations generated in the scenarios of (b1) and (b2). The dashed lines indicate the left and right sides of the target area, divided by the center 0; in the scenario of (b2), the observation locations on the left side are sparse.

Table 1 shows the scenarios for the numerical studies. The scenario combining setting (a3) and (b2) is the same as the scenario with the rotated region in setting 3 and is omitted in these numerical studies because it does not affect the weights used to estimate coefficients. The situation assumed for GWR and BGWR is Scenario 1; the situations assumed for BGWSR are Scenarios 2, 4, and 5.



(a) Scenario (b1)

(b) Scenario (b2)

Figure 2: Examples of observation locations for each scenario

Table 1: Scenarios

	true values of coefficients	Left-right ratio of observation locations (Whether there is sparse or dense)
Scenario1	smoothly (a1)	1 : 1 (b1)
Scenario2	smoothly (a1)	1 : 4 (b2)
Scenario3	left and right clusters (a2)	1 : 1 (b1)
Scenario4	left and right clusters (a2)	1 : 4 (b2)
Scenario5	upper and lower clusters (a3)	1 : 4 (b1)

3.2 Comparative methods and Hyperparameters settings

We use our proposed method, BGWSR, and the existing methods, GWR and BGWR, in the numerical studies. We apply two BGWSR methods: BGWSR with Adjacency Estimation (BGWSR-AE), which determines the adjacency range differently for each location, and BGWSR, which uses a common adjacency range for all locations. We set the hyperparameters in BGWSR and BGWSR-AE as follows:

$$(r, q, r_1, q_1, r_2, q_2, a)' = (0.1, 0.1, 0.1, 0.1, 0.1, 0.1, 3)'.$$

The parameters $r_{\text{BGWR}}, q_{\text{BGWR}}$ for the prior distribution of the error variance σ^2 in BGWR were similarly set by

$$(r_{\text{BGWR}}, q_{\text{BGWR}})' = (0.1, 0.1)'.$$

The method for determining the adjacent locations of BGWR is based on Ma et al. (2021), sampling the bandwidth h_{BGWR} using the MH method. The prior distribution of h_{BGWR} is the following Uniform distribution.

$$h_{\text{BGWR}} \sim U(0, 3).$$

We selected $\{0.10, 0.15, \dots, 3.00\}$ as the candidate bandwidth h_{GWR} in GWR and determined it using 5-fold cross validation.

3.3 Performance measures

We evaluate in the numerical studies the estimation performance of the coefficients and objective variable at the observed and prediction location. We use the mean squared error (MSE) as the performance measure and define the

MSE at the observation location as

$$\frac{1}{n} \sum_{i=1}^n \left(\widehat{\beta}_k(\mathbf{s}_i) - \beta_k(\mathbf{s}_i) \right)^2,$$

$$\frac{1}{n} \sum_{i=1}^n \left(\widehat{y}(\mathbf{s}_i) - y(\mathbf{s}_i) \right)^2,$$

where $\widehat{\beta}(\mathbf{s}_i) = (\widehat{\beta}_1, \widehat{\beta}_2, \dots, \widehat{\beta}_p)'$, $\widehat{y}(\mathbf{s}_i)$ are the estimated value of the coefficients and the objective variable at observed locations; $\beta(\mathbf{s}_i)$, $y(\mathbf{s}_i)$ are the true value of the coefficient and the objective variables at observed locations. The MSE at the prediction location is defined as

$$\frac{1}{n^*} \sum_{i^*=1}^{n^*} \left(\widehat{\beta}_k(\mathbf{s}_{i^*}) - \beta_k(\mathbf{s}_{i^*}) \right)^2,$$

$$\frac{1}{n^*} \sum_{i^*=1}^{n^*} \left(\widehat{y}(\mathbf{s}_{i^*}) - y(\mathbf{s}_{i^*}) \right)^2,$$

where $\mathbf{s}_{i^*} \in D$ is the prediction location, and $\widehat{\beta}(\mathbf{s}_{i^*})$, $\widehat{y}(\mathbf{s}_{i^*})$ are the predicted value of the coefficients and the objective variables at prediction location \mathbf{s}_{i^*} . The true value of the coefficient at location \mathbf{s}_{i^*} is $\beta(\mathbf{s}_{i^*})$, and that of the objective variable is $y(\mathbf{s}_{i^*})$.

3.4 Summary of Numerical Studies Results

In the numerical studies, we generated data for each scenario 10 times each and calculated the median of the resulting evaluation metrics for each method applied. Table 2 shows the median MSE for each method.

In Scenario 1, with respect to the MSE for the observation locations, the BGWSR performed the best for the objective variables and some of the coefficients, and the BGWSR-AE performed equally well. Similarly, for the MSE for the prediction location, the BGWSR performed best, and the BGWSR-AE performed equally well for the objective variables and most of the coefficients. Figure 3 shows an example of the true values of the coefficients and the estimates generated by each method for the location of the observation in Scenario 1. BGWSR-AE tended to produce estimates closer to the overall average rather than abrupt changes in the coefficients. This is because the application of Bayesian Fused Lasso fails to capture the rapid changes.

In Scenario 2, for the MSE for the observation locations, BGWSR-AE yielded the best results for the objective variables and some coefficients. Based on the results of the MSE for the prediction locations, BGWSR-AE and BGWSR had a high performance for the objective variables and coefficients. In Scenario 2, BGWSR-AE and BGWSR can guarantee the similarity of locations by Bayesian Fused Lasso. Figure 4 shows an example of the true values of the coefficients and the estimated values by each method for the two locations in Scenario 2. BGWSR-AE and BGWSR estimate values close to the true values even in regions where observed locations are sparse. BGWR and GWR have locations with extremely large estimated values in sparse areas. This is because the BGWR and GWR set the range of adjacent locations to be relatively small to match the dense locations. Consequently, extreme values are estimated for locations where the data size is small.

In Scenario 3, BGWSR-AE and BGWSR exhibited high performance for objective variables and coefficients at the observed location. According to the MSE for the prediction location, the BGWSR performed the best for the objective variables and coefficients. Figure 5 shows the true values of the coefficients for the observation locations for Scenario 3 and examples of the estimated values for each method. Scenario 3 has a cluster structure for locations, suggesting that BGWSR-AE and BGWSR can estimate coefficients more uniformly within clusters than the other methods. However, there are many locations where the coefficients are shrunk to 0 as a whole compared to the true values. Nevertheless, in the BGWR, the estimation is unstable near the edge of the cluster. For the GWR, the estimated coefficients varied gently near the edge of the cluster and within clusters. This suggests that the estimation performance of BGWR and GWR deteriorates near cluster boundaries.

In Scenario 4, BGWSR-AE had high performance for the objective variables and coefficients at the observation locations. For the MSE for the prediction location, the BGWSR-AE performed the best for the objective variables and most of the coefficients, and the BGWSR performed equally well. Figure 6 shows an example of the true values of the coefficients and the estimates generated by each method in Scenario 4. The results suggest that BGWSR-AE and BGWSR can estimate similarity coefficients within clusters compared to the other methods. Additionally, BGWSR-AE and BGWSR provide numerically stable coefficients even in areas with sparse observation locations. This suggests

that the Bayesian Fused Lasso effectively considers the similarity of adjacent locations. Nonetheless, for the BGWR and GWR, the estimation became unstable near the edge of the cluster. In areas with sparse observation locations, extremely large or small coefficients were predicted due to the small data size.

In Scenario 5, relative to the MSE for the observation locations, BGWSR-AE, and BGWSR had high performance on the objective variables and coefficients at the observation locations. BGWSR performed the best for the prediction locations. Meanwhile the GWR yielded the best results on the objective variables, and the BGWSR performed similarly well. Figure 7 shows an example of the true values of the coefficients and the estimated values produced by each method in Scenario 5. The results suggest that BGWSR-AE and BGWSR can estimate coefficients more similarly within clusters than BGWR and GWR. For BGWSR-AE, BGWSR, and GWR, the prediction of coefficients in the upper clusters yielded larger estimates compared to the true values across clusters due to Bayesian Fused Lasso. For BGWR and GWR, the coefficient estimates were unstable at the edge of the domain and in areas with sparse observation locations.

Table 2: Median MSE for each method

senario	method	observation location				prediction location			
		β_1	β_2	β_3	y	β_1	β_2	β_3	y
1	BGWSR-AE	0.025	0.052	0.027	0.037	0.037	0.057	0.042	0.189
	BGWSR	0.024	0.051	0.027	0.036	0.032	0.068	0.033	0.161
	BGWR	0.046	0.083	0.044	0.167	0.041	0.075	0.037	0.187
	GWR	0.033	0.027	0.035	0.110	0.046	0.035	0.046	0.164
2	BGWSR-AE	0.024	0.041	0.027	0.032	0.042	0.057	0.059	0.172
	BGWSR	0.032	0.040	0.031	0.032	0.046	0.062	0.056	0.165
	BGWR	0.046	0.054	0.034	0.156	0.048	0.068	0.065	0.180
	GWR	0.057	0.036	0.047	0.119	0.152	0.064	0.219	0.323
3	BGWSR-AE	0.045	0.031	0.048	0.054	0.070	0.083	0.080	0.223
	BGWSR	0.036	0.028	0.052	0.055	0.056	0.049	0.059	0.145
	BGWR	0.077	0.075	0.089	0.199	0.057	0.060	0.078	0.187
	GWR	0.046	0.044	0.065	0.167	0.081	0.068	0.068	0.259
4	BGWSR-AE	0.034	0.041	0.031	0.052	0.085	0.086	0.088	0.293
	BGWSR	0.053	0.054	0.048	0.053	0.088	0.095	0.089	0.306
	BGWR	0.090	0.062	0.084	0.224	0.109	0.094	0.078	0.345
	GWR	0.052	0.071	0.049	0.210	0.090	0.139	0.114	0.400
5	BGWSR-AE	0.045	0.040	0.053	0.039	0.078	0.086	0.104	0.278
	BGWSR	0.033	0.036	0.033	0.039	0.058	0.052	0.064	0.164
	BGWR	0.073	0.064	0.074	0.157	0.075	0.069	0.068	0.196
	GWR	0.049	0.047	0.078	0.142	0.067	0.074	0.088	0.160

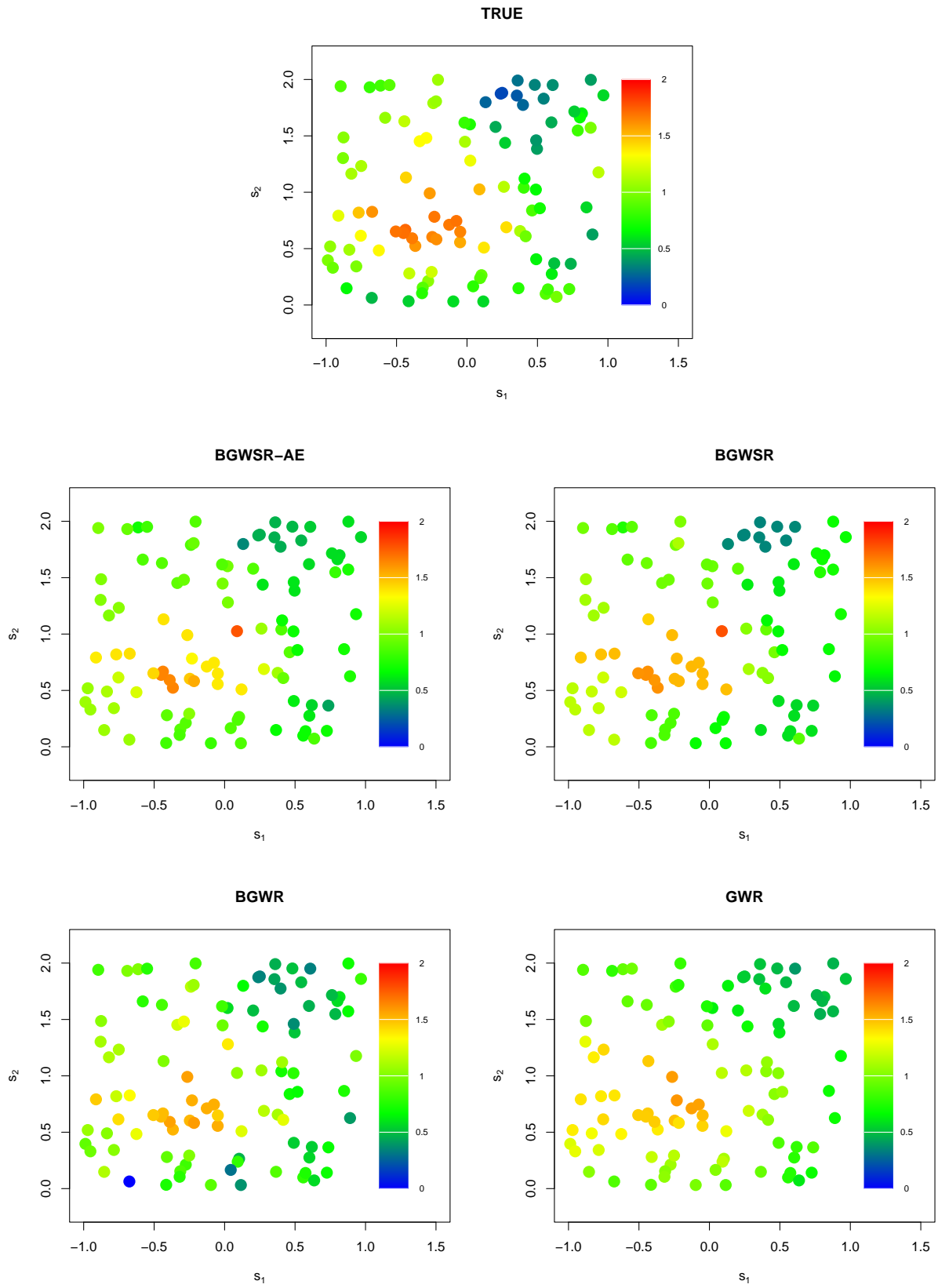


Figure 3: True and estimated values of coefficients for observation locations in Scenario 1

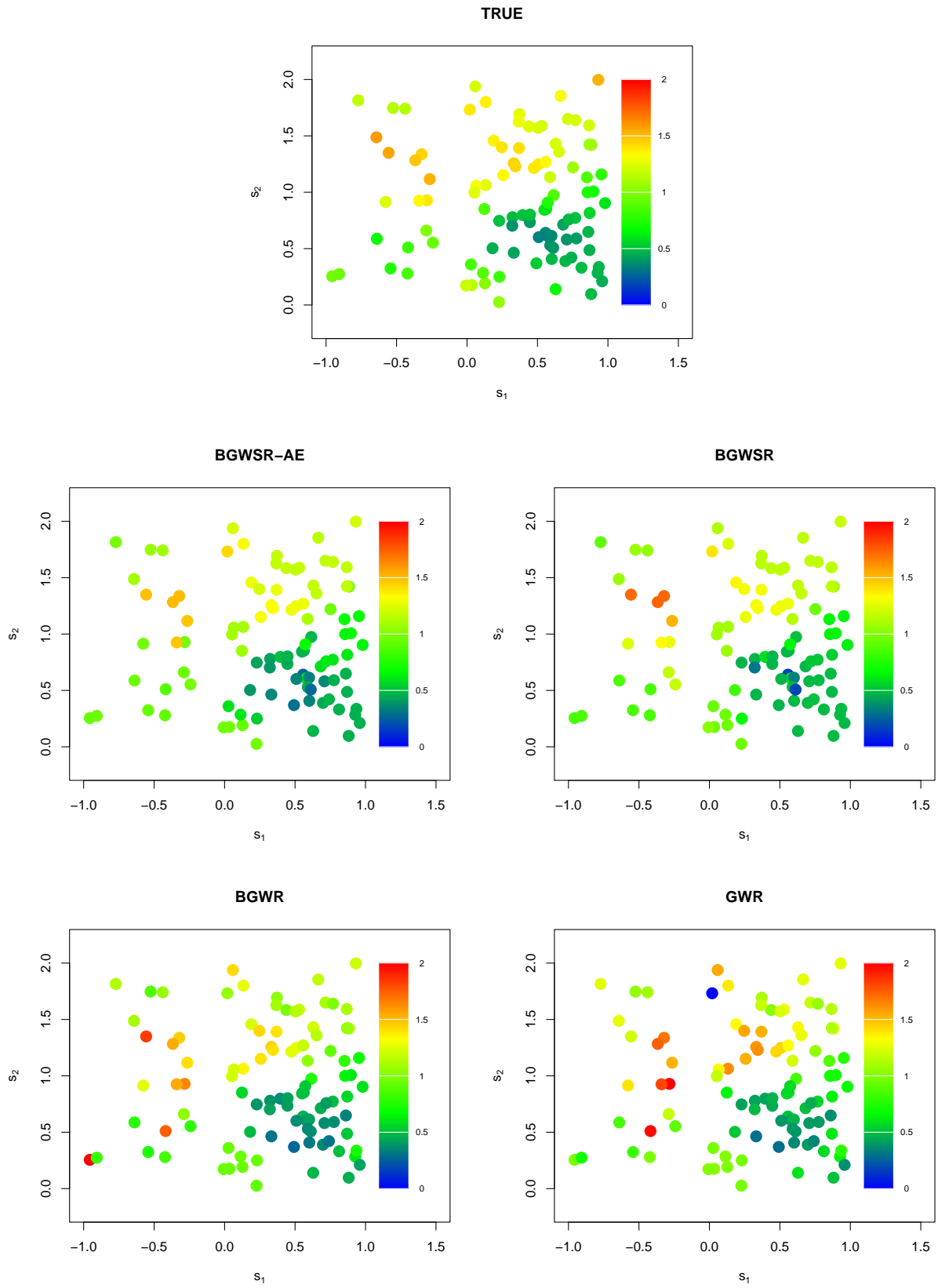


Figure 4: True and estimated values of coefficients for observation locations in Scenario 2

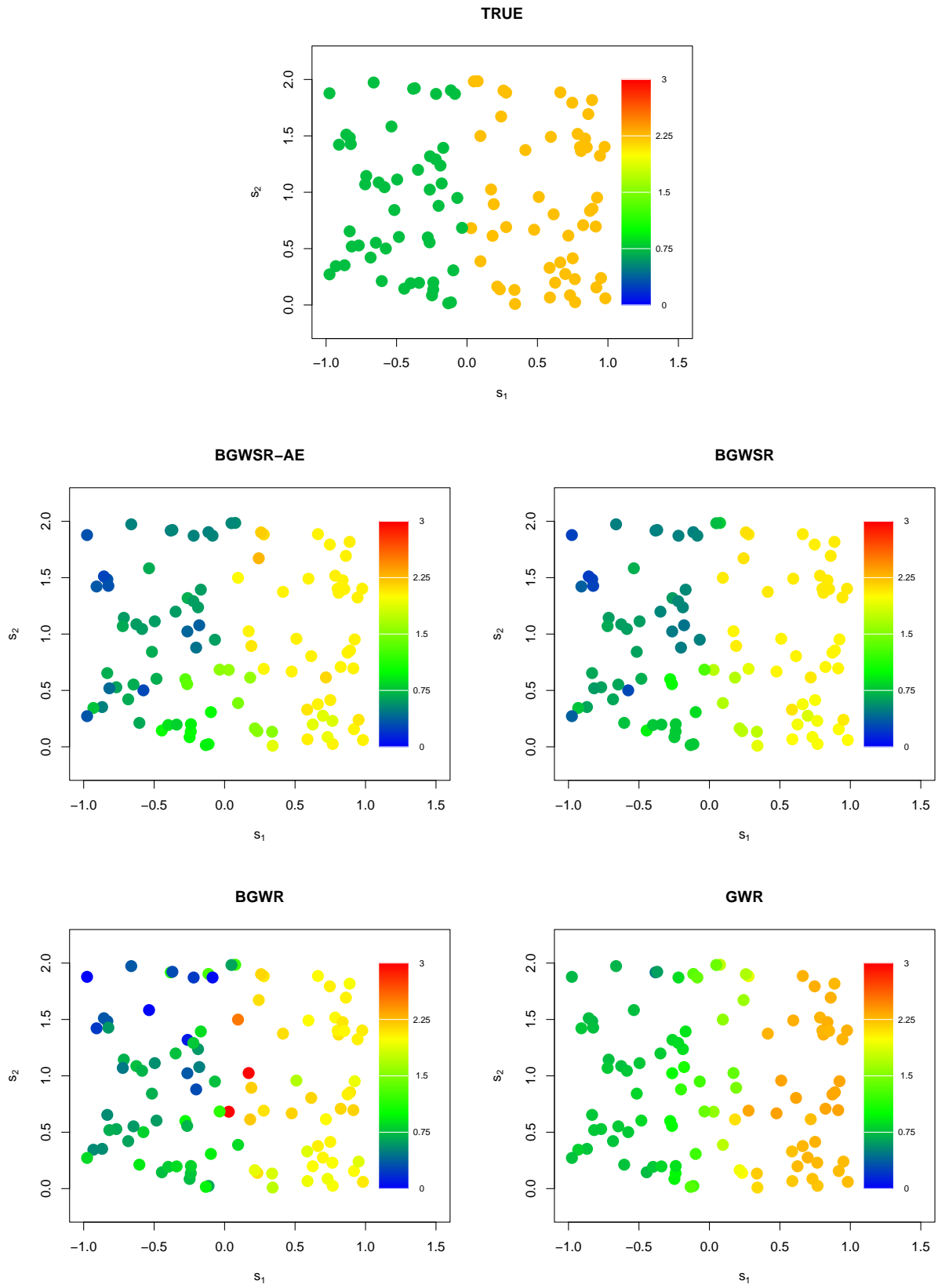


Figure 5: True and estimated values of coefficients for observation locations in Scenario 3

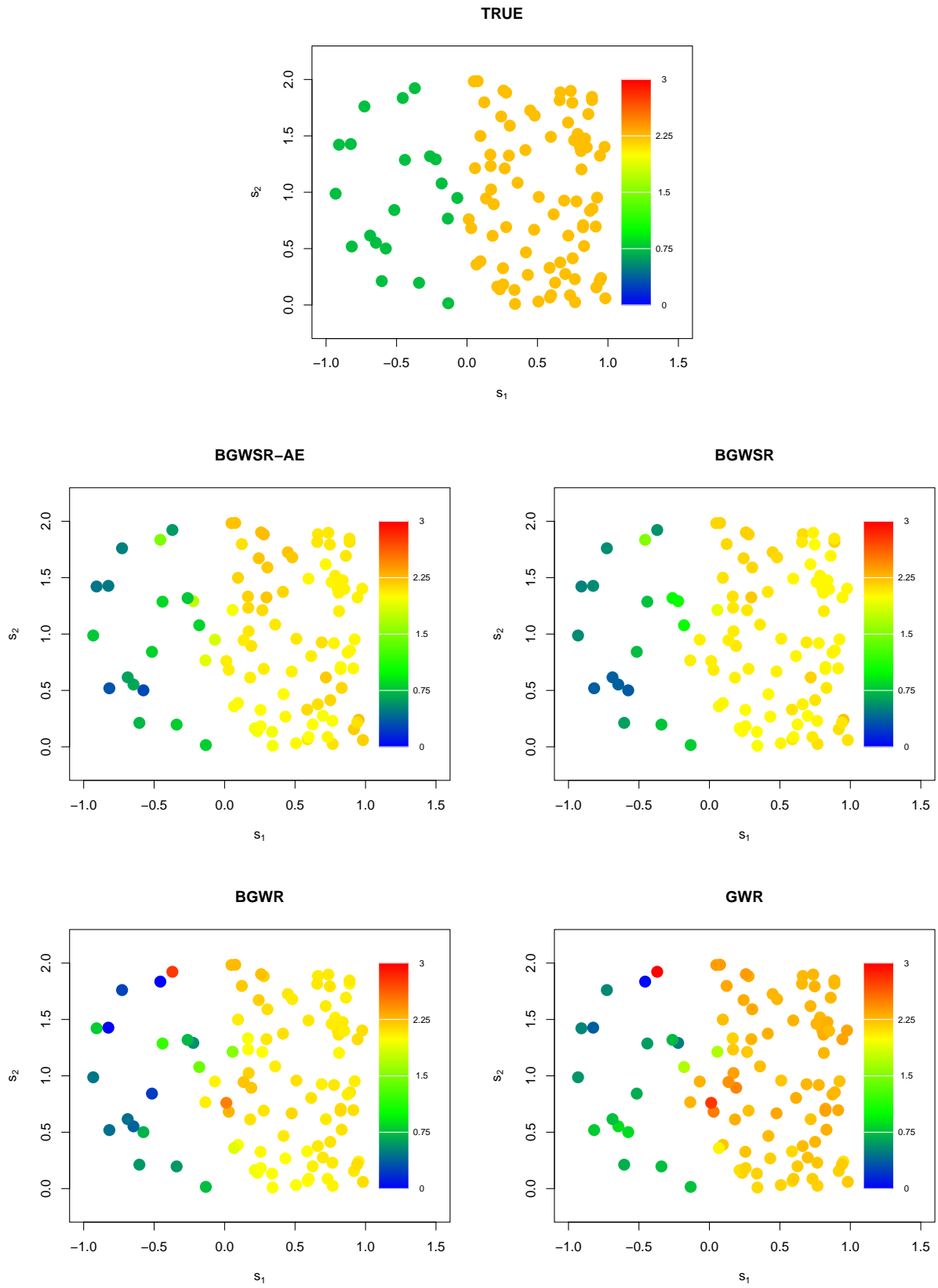


Figure 6: True and estimated values of coefficients for observation locations in Scenario 4

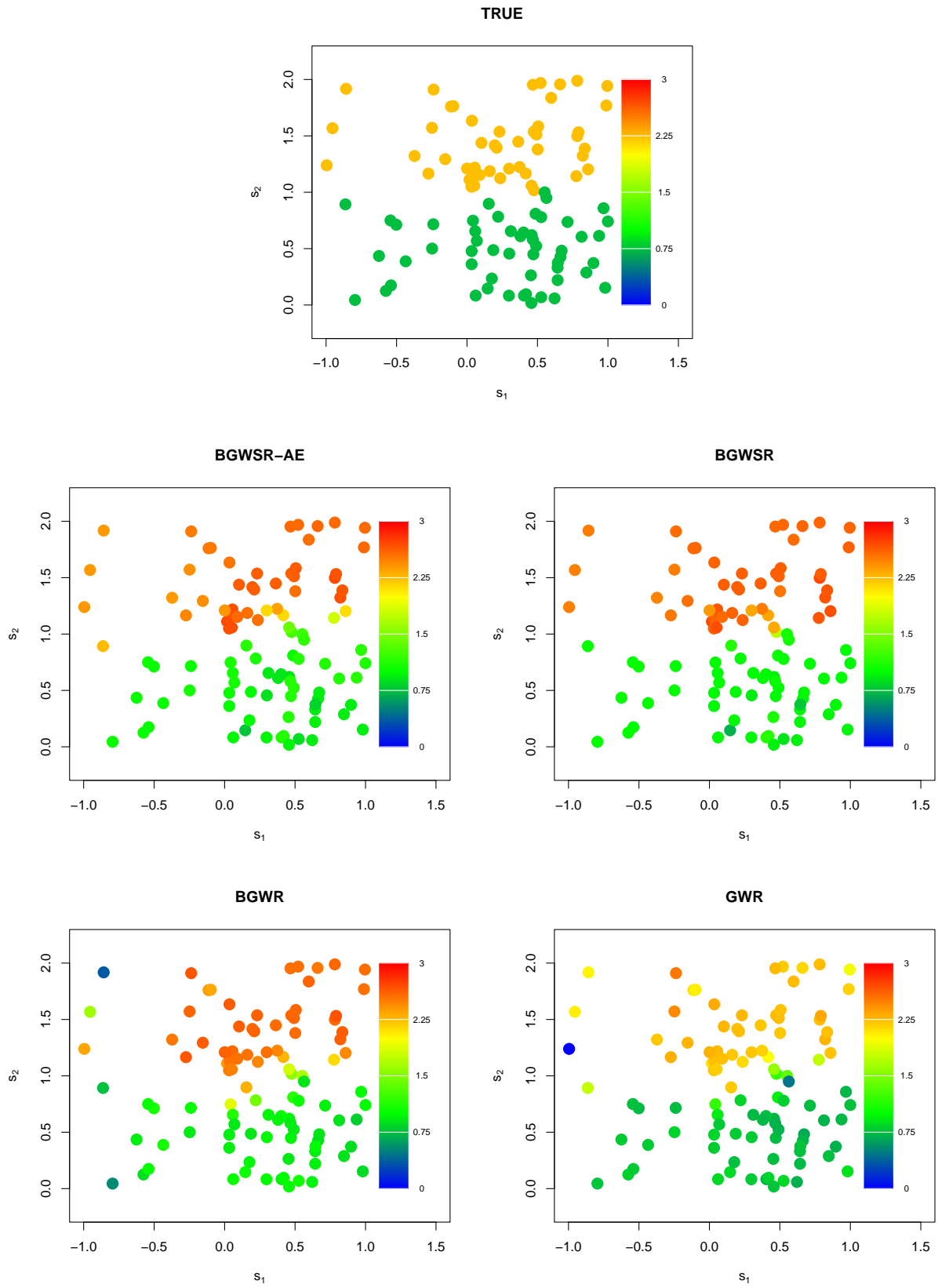


Figure 7: True and estimated values of coefficients for observation locations in Scenario 5

4 Application to land price data

In this section, we evaluate the prediction performance of the proposed method by applying it to real data to demonstrate its usefulness.

4.1 Data Summary and Applicable Settings

The data used are the official land price data for Tokyo for the year 2021, published by the Ministry of Land, Infrastructure, Transport and Tourism (Ministry of Land and Tourism, 2021). The data were obtained for 1219 locations, and 114 variables such as land use classification and type of frontage road were obtained based on the location information of latitude and longitude. Figure 8 plots the obtained data by location information and shows the land prices in 2021 in colors. In this study, we randomly selected 130 locations in the area around the city center, which is surrounded by the black square in Figure 8. Subsequently, we randomly selected 100 observation locations and 50 prediction locations. Figure 9 shows the observation locations and prediction locations. The observation locations are mostly available in the left half of the city center, while the data are less available in the right half of the city center—the data are coarse-grained in terms of observation locations. The variables used are shown in table 3. In this application, latitude and longitude were used as location, price as the objective variable, and the volume ratio, land area, and station distance as explanatory variables.

Table 3: List of variables used in real data example

	variables	details
location	latitude	Y -coordinate obtained by World Geodetic System (sec)
	longitude	X -coordinate obtained by World Geodetic System (sec)
objective variable	price	land prices in 2021 (Yen/m ² , Yen/10a for forest land)
covariates	floor area ratio	Ratio of total building area (total floor space) to site area (%)
	land area	land area (m ²)
	distance	Distance to the nearest station (m)

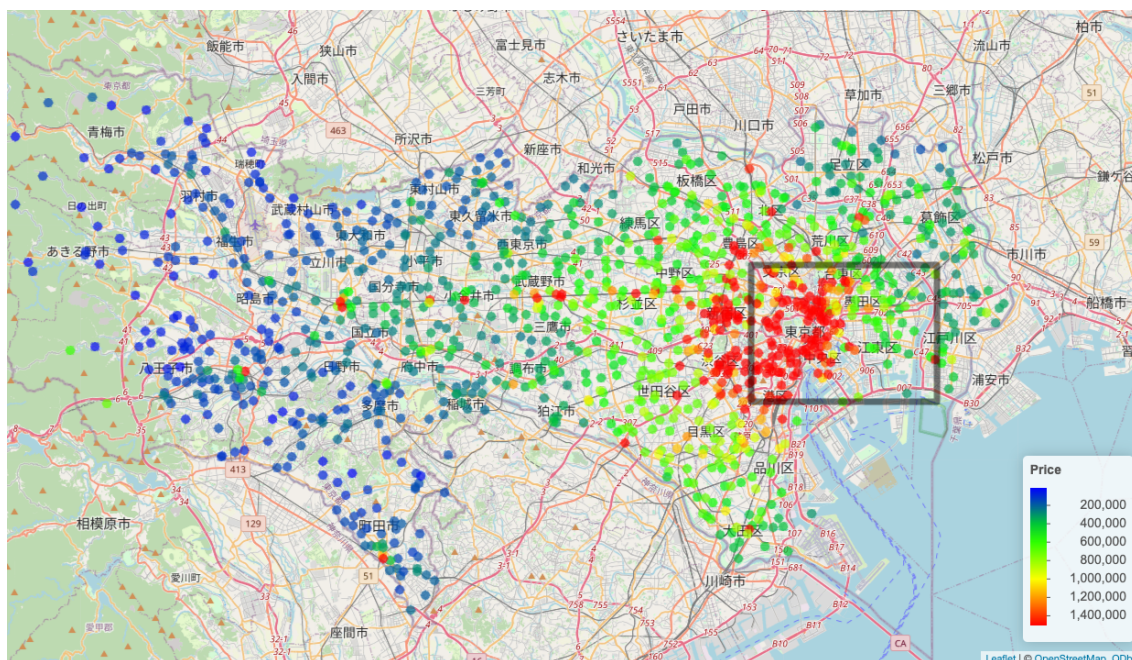


Figure 8: land price in Tokyo



Figure 9: Locations used in the analysis

We set up the hyperparameters for each method and the method of determining the neighboring locations in the same way as in the numerical studies of refchap:numerical study.

4.2 Results

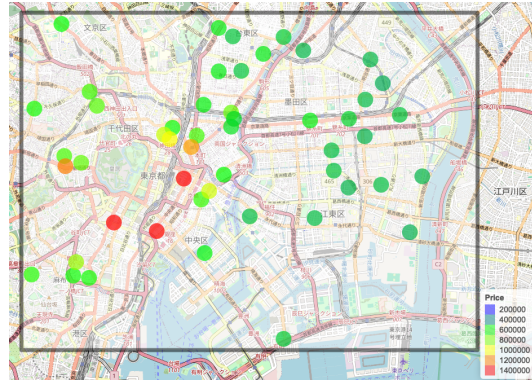
Table 4 shows the MSE of the objective variable prediction by each method at the prediction location. The MSE of BGWSR was the smallest. It was followed by BGWSR-AE with the smallest MSE and GWR with the largest MSE. Figure 10 shows the true value of the price at the prediction location and the predicted value by each method, colored according to the magnitude of the value and visualized on the map. As shown in Figure 10, BGWSR-AE produced the closest prediction to the true value. Compared to the other methods, BGWSR-AE did not produce extremely small values as predictions, suggesting that the Bayesian Lasso effect stabilizes the estimated values. However, BGWSR and GWR produced predictions that were extremely large or small compared to the true value in the vicinity of the city center and near the boundaries of the region.

Table 5 shows the estimated coefficients for each method at the observation location, colored according to the magnitude of the value and visualized on a map. The β_1 , β_2 , β_3 are the coefficients for the floor area ratio, land area, and distance. First, focusing on the estimated coefficients for the floor area ratio, the coefficients are large in the city center and decrease gradually as one moves away from the city center, as is the case for all the methods. For BGWSR-AE and BGWSR, the coefficients were estimated to vary gradually around the city center. Nevertheless, for BGWSR and GWR, the estimated coefficients differed between the city center and areas far from it. Next, focusing on the estimated coefficients for land area, all the methods had a negative value for the coefficient in urban centers. However, the coefficients of BGWSR, BGWR, and GWR are close to -1 in the city center, while those of BGWSR-AE are around 0.4 . Finally, in the BGWSR-AE, the estimated coefficients for station distance were larger near Chiyoda-ku and smaller away from there. Nonetheless, for BGWSR, BGWR, and GWR, the coefficients were estimated to be large in the upper right of the region and decreased toward the lower left.

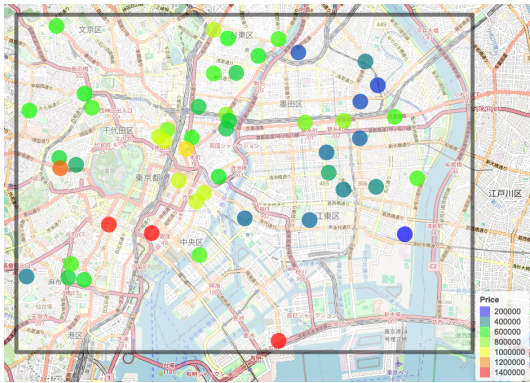
Figure 11 shows a visualization of the predicted values of the objective variable by BGWSR-AE, BGWSR, and BGWR, colored by the size of the range of the 95% credible interval. From Figure 11, BGWSR-AE and BGWSR have more locations with smaller interval widths compared to BGWR. In particular, the interval widths were smaller for BGWSR-AE and BGWSR even at the edge of the region. The ratio of true values included in the 95% confidence interval was the same for all methods. This suggests that BGWSR-AE and BGWSR have less uncertainty than BGWR. Furthermore, BGWSR-AE and BGWSR are useful because they have smaller MSEs than BGWR and GWR.

Table 4: MSE of predicted and true values

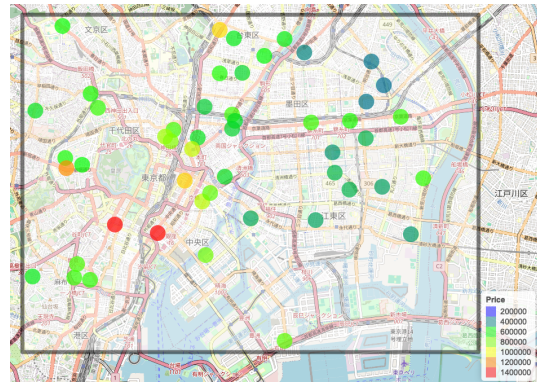
method	MSE_y
BGWSR-AE	0.092
BGWSR	0.082
BGWR	0.135
GWR	0.171



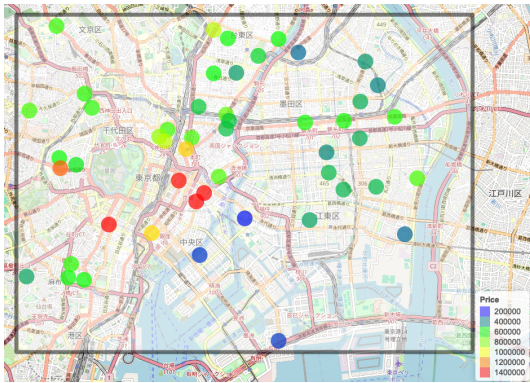
(a) TRUE



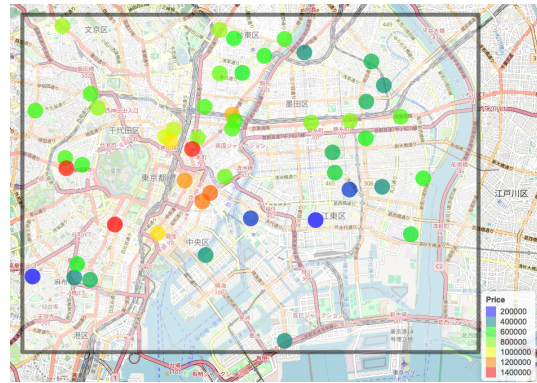
(b) BGWSR-AE



(c) BGWSR



(d) BGWR



(e) GWR

Figure 10: True and predicted price at the prediction location

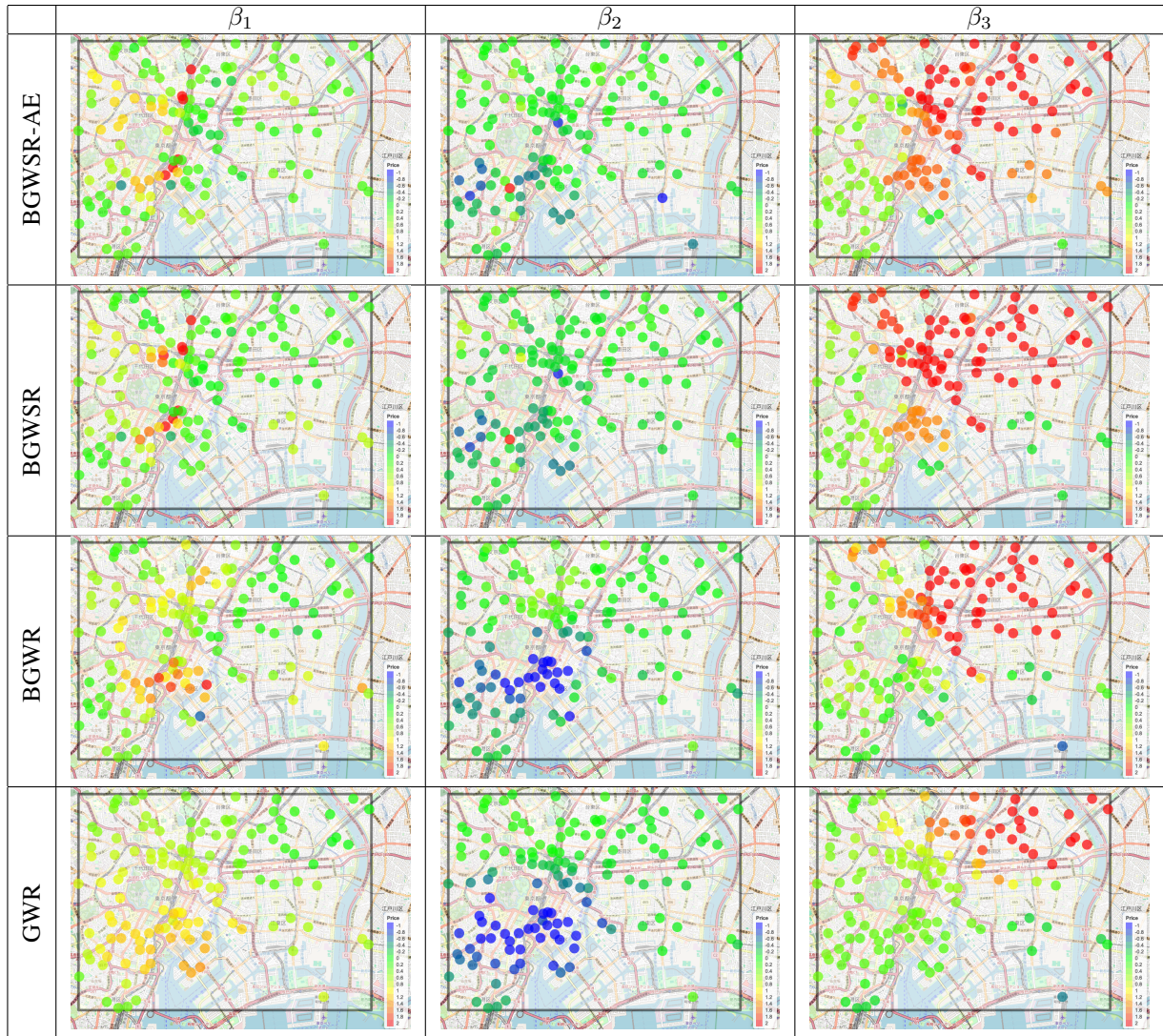


Table 5: Estimated coefficients at observation locations

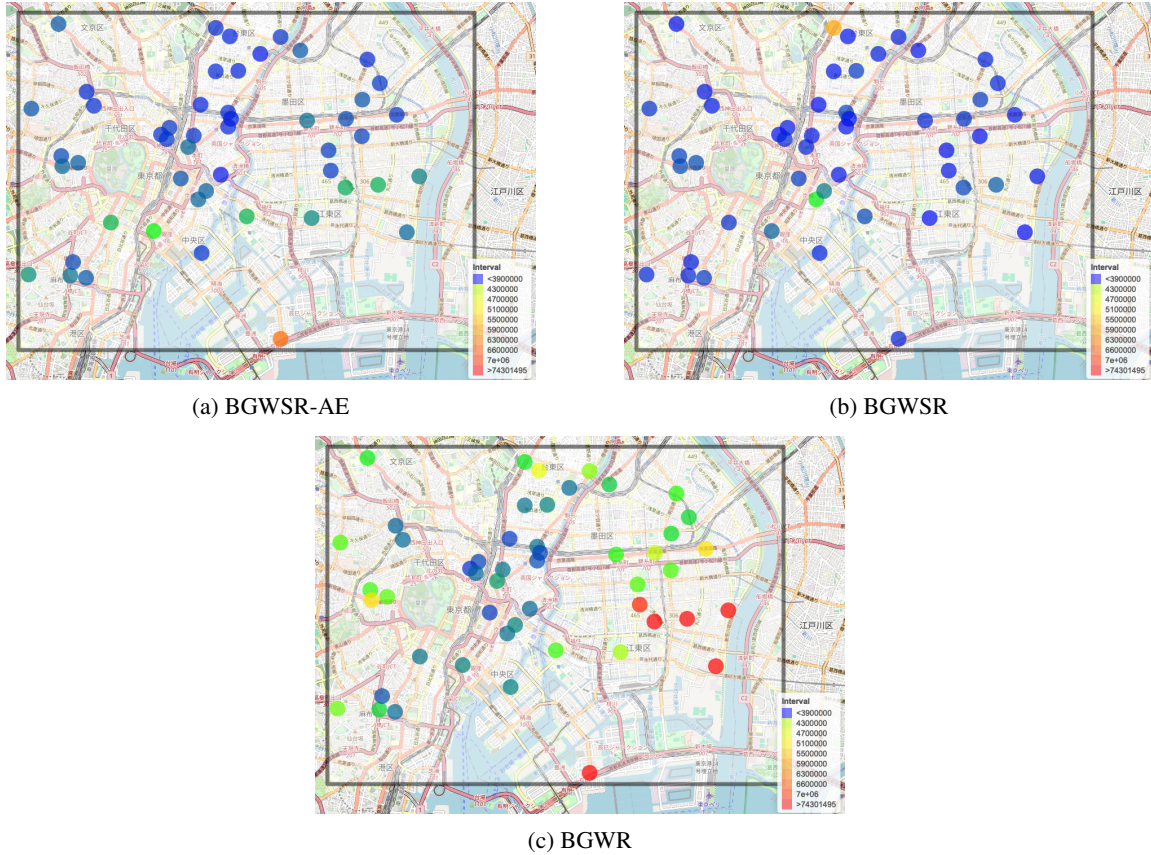


Figure 11: the Range of Credible interval of price at the prediction location

5 Conclusion

This paper proposes a BGWSR by combining the idea of Bayesian Fused Lasso and BGWR. The proposed method enables us to consider spatial correlations even when the number of observation locations is small. Moreover, by introducing a method of determining the range of adjacent locations for each location into BGWSR, the prediction performance is effectively maintained even when the observation locations are heterogeneous.

This paper shows the usefulness of the proposed method through numerical studies. The results show that the proposed method has better prediction performance for the coefficients and the objective variable compared to estimated by GWR and BGWR, where observation locations are obtained heterogeneously in space. The results suggest that the proposed method effectively considers the similarity of the coefficients between adjacent locations since the estimated values of the coefficients are close among the adjacent locations. Furthermore, when the locations have a cluster structure, the estimated values of the proposed method are the same coefficients within the clusters. We also applied the existing and proposed methods to land price data for Tokyo, where the density of observation locations was spatially heterogeneous. The results showed that the proposed method performed better than the existing methods in predicting the objective variables. Furthermore, we evaluated the uncertainty of the predicted values of the objective variables. Consequently, we confirmed that the proposed method has a smaller 95% credible interval than BGWR, even at the edge of the domain and in areas with sparse observation locations, and that most locations include the true value within the interval. The results suggest that the proposed method has less uncertainty than BGWR.

The proposed method can be widely used for data obtained from heterogeneous observation patterns of location, and when spatial autocorrelation is assumed in the coefficients. For example, the soil data used in Koh et al. (2020) have observation locations where there are sparse and dense densities of locations. In addition, data for seismic intensity observation locations in earthquake intensity prediction and infection status in epidemiology are often obtained in a spatially heterogeneous pattern. The proposed method is thus useful for such data.

BGWSR could be potentially improved in several aspects. First, it is necessary to find a way to determine the function of the weights used to estimate the adjacency locations. The numerical studies and real data examples presented in this

paper use Bi-square, but existing studies have proposed Boxcar, Gaussian, and other weight functions (Fotheringham et al., 2003). It is necessary to select the appropriate approach among these weighting function based on the characteristics of the data to be applied. For example, when using Boxcar, the predicted values of the coefficients tend to be similar across the whole set. If the purpose of the estimation is to emphasize the mean structure of the coefficients, the use of Boxcar therefore may be appropriate.

The second point of potential improvement is enhancing interpretability for high-dimensional data. BGWSR uses a Laplace distribution for the prior distribution of the coefficients. Hence, the estimates of the coefficients are not exactly 0 in the methods that use the posterior mean or posterior median as the estimator of the coefficient. This may reduce interpretability. In the case of multivariate data analysis, variable selection methods are often used and known to improve interpretability (Tibshirani, 1996). For achieving this issue, one of the directions is the use of Horseshoe prior for the prior distribution (Carvalho et al., 2010), and Spike and Slab prior (Ročková and George, 2018). This allows to drive the estimation of some coefficient estimates to 0 and is expected to improve interpretability. For BGWSR, similarly changing the prior distribution is expected to improve interpretability through variable selection when applied to high-dimensional data.

References

- Ahmed, S. and De Marsily, G.(1987). Comparison of geostatistical methods for estimating transmissivity using data on transmissivity and specific capacity, *Water Resources Research*, **23**(9), 1717–1737.
- Andrews, D. F. and Mallows, C. L.(1974). Scale mixtures of normal distributions, *Journal of the Royal Statistical Society: Series B (Methodological)*, **36**(1), 99–102.
- Bailey, T. C., Gatrell, A. C. et al.(1995). *Interactive Spatial Data Analysis*, Longman Scientific & Technical Essex, England.
- Boehm Vock, L. F., Reich, B. J., Fuentes, M., and Dominici, F.(2015). Spatial variable selection methods for investigating acute health effects of fine particulate matter components, *Biometrics*, **71**(1), 167–177.
- Brunsdon, C., Fotheringham, A. S., and Charlton, M. E.(1996). Geographically weighted regression: A method for exploring spatial nonstationarity, *Geographical Analysis*, **28**(4), 281–298.
- Carvalho, C. M., Polson, N. G., and Scott, J. G.(2010). The horseshoe estimator for sparse signals, *Biometrika*, **97**(2), 465–480.
- Cline, A. K.(1973). Curve fitting using splines under tension(Curve fitting by application of splines under tension, discussing polynomial interpolation drawbacks and linear system solution for unknown second derivatives), *Atmospheric Technology*, **3**, 60–65.
- Fischer, M. M. and Getis, A.(2010). *Handbook of Applied Spatial Analysis: Software Tools, Methods and Applications*, Springer, New York.
- Fotheringham, A. S., Brunsdon, C., and Charlton, M.(2003). *Geographically Weighted Regression: the Analysis of Spatially Varying Relationships*, John Wiley & Sons, New York.
- Fotheringham, A. S., Yang, W., and Kang, W.(2017). Multiscale geographically weighted regression (MGWR), *Annals of the American Association of Geographers*, **107**(6), 1247–1265.
- Jena, R., Pradhan, B., Gite, S., Alamri, A., and Park, H.-J.(2023). A new method to promptly evaluate spatial earthquake probability mapping using an explainable artificial intelligence (XAI) model, *Gondwana Research*, **123**, 54–67.
- Koh, E.-H., Lee, E., and Lee, K.-K.(2020). Application of geographically weighted regression models to predict spatial characteristics of nitrate contamination: Implications for an effective groundwater management strategy, *Journal of Environmental Management*, **268**, 110646.
- Krige, D. G.(1951). A statistical approach to some basic mine valuation problems on the Witwatersrand, *Journal of the Southern African Institute of Mining and Metallurgy*, **52**(6), 119–139.
- Kyung, M., Gill, J., Ghosh, M., and Casella, G.(2010). Penalized regression, standard errors, and bayesian lassos, *Bayesian Analysis*, **5**(2), 369–412.
- Ministry of Land, T., Infrastructure and Tourism(2021). National Land Price Information (Land Price Public Notice Data), . https://nlftp.mlit.go.jp/ksj/gml/datalist/KsjTmplt-L01-v3_0.html (acquired in 26/12/2023).

- LeSage, J. P.(2004). A family of geographically weighted regression models, in *Advances in Spatial Econometrics: Methodology, Tools and Spplications*, Springer, Berlin Heidelberg, 241–264.
- Li, F. and Sang, H.(2019). Spatial Homogeneity Pursuit of Regression Coefficients for Large Datasets, *Journal of the American Statistical Association*, **114**(527), 1050–1062.
- Ma, Z., Xue, Y., and Hu, G.(2021). Geographically weighted regression analysis for spatial economics data: A Bayesian recourse, *International Regional Science Review*, **44**(5), 582–604.
- Park, T. and Casella, G.(2008). The Bayesian lasso, *Journal of the American Statistical Association*, **103**(482), 681–686.
- Ročková, V. and George, E. I.(2018). The spike-and-slab lasso, *Journal of the American Statistical Association*, **113**(521), 431–444.
- Subedi, N., Zhang, L., and Zhen, Z.(2018). Bayesian geographically weighted regression and its application for local modeling of relationships between tree variables, *iForest-Biogeosciences and Forestry*, **11**(5), 542.
- Tibshirani, R.(1996). Regression shrinkage and selection via the lasso, *Journal of the Royal Statistical Society: Series B (Methodological)*, **58**(1), 267–288.
- Tibshirani, R., Saunders, M., Rosset, S., Zhu, J., and Knight, K.(2005). Sparsity and smoothness via the fused lasso, *Journal of the Royal Statistical Society: Series B (Methodological)*, **67**(1), 91–108.
- Wang, X., Zhu, Z., and Zhang, H. H.(2023). Spatial heterogeneity automatic detection and estimation, *Computational Statistics & Data Analysis*, **180**, 107667.
- Yu, D., Wei, Y. D., and Wu, C.(2007). Modeling spatial dimensions of housing prices in Milwaukee, WI, *Environment and Planning B: Planning and Design*, **34**(6), 1085–1102.
- Zhong, Y., Sang, H., Cook, S. J., and Kellstedt, P. M.(2023). Sparse spatially clustered coefficient model via adaptive regularization, *Computational Statistics & Data Analysis*, **177**, 107581.